The (^{54}Fe+^{58}Ni)/^{56}Ni ratio as a second parameter for Type Ia supernova properties

Paolo A. Mazzali[1,2]⋆ and Philipp Podsiadlowski[3]

[1]*Max-Planck Institut für Astrophysik, Karl-Schwarzschildstr. 1, 85748 Garching, Germany*
[2]*Istituto Naz. di Astrofisica-Oss. Astron., Via Tiepolo, 11, 34131 Trieste, Italy*
[3]*Department of Astronomy, Oxford University, Oxford, OX1 3RH*

ABSTRACT

A variation of the relative content of (^{54}Fe+^{58}Ni) versus ^{56}Ni may be responsible for the observed scatter of Type Ia supernovae (SNe Ia) about a mean relation between their intrinsic brightness and the shape of their light curve. Synthetic light curves are computed from parametrized Chandrasekhar-mass explosion models of constant kinetic energy, where the ejecta are divided into an inner nuclear statistical equilibrium (NSE) zone, composed of (^{54}Fe+^{58}Ni) inside and ^{56}Ni outside, an outer zone with intermediate-mass elements, and a CO zone. Both the size of the NSE zone and the fraction of (^{54}Fe+^{58}Ni) versus ^{56}Ni are varied systematically. Models with the same original NSE content but different (^{54}Fe+^{58}Ni)/^{56}Ni ratios reach different peak brightness but have similar light curve shapes. Synthetic spectra indicate that the *V*-band decline rate is not affected by the (^{54}Fe+^{58}Ni)/^{56}Ni ratio. While the ^{56}Ni mass and the total NSE mass are the dominant parameters that determine the peak luminosity and the shape of the light curve, respectively, a variation in the (^{54}Fe+^{58}Ni)/^{56}Ni ratio, which may depend on the metallicity of the progenitor is likely to account for a significant part of the observed scatter of local SNe Ia about the mean brightness–decline rate relation.

Key words: supernovae: general.

1 INTRODUCTION

The use of Type Ia supernovae (SNe Ia) to constrain cosmological parameters relies on the calibration of their luminosity. Although SNe Ia are not standard candles, several of their observed properties can be linked to their peak brightness. These properties include the decline in *B*-band magnitude in the first 15 d after *B* maximum, $\Delta m_{15}(B)$ (Phillips 1993; Phillips et al. 1999), the shape of the light curve [e.g. Multi-Colour Light Curve Shape (see Riess et al. 1998), 'stretch' (see Perlmutter et al. 1997)], the ratio of two Si II lines (Nugent et al. 1995), the width of the nebular emission lines (Mazzali et al. 1998), the Hubble type of the parent galaxy (Hamuy et al. 2000; Branch, Romanishin & Baron 1996; van den Bergh 1997; van den Bergh, Li & Filippenko 2005), the distance from the centre of the host galaxy (Wang, Höflich & Wheeler 1997), and the $B - V$ colour $\sim$12 d after *B* maximum (Wang et al. 2005).

All these relations indicate that the properties of SNe Ia are determined by one dominant, driving parameter, which should be closely related to the amount of ^{56}Ni synthesized in the explosion (Höflich et al. 1996). However, scatter about the mean relation is always present. This scatter may be due to uncertainties in distance and

reddening affecting the estimate of the SN brightness, but it remains even when distance- and reddening-free quantities are used [e.g. nebular line width versus $\Delta m_{15}(B)$; Mazzali et al. 1998]. Apart from possible uncertainties in the measurements, this scatter suggests that a single parameter is not sufficient to describe all possible variations of the SN Ia phenomenon. This has also been confirmed by detailed studies of individual SNe (Benetti et al. 2004).

The observed scatter could be due to a number of factors, which may in turn be related to properties of the progenitor system (e.g. distribution of ^{56}Ni in the ejecta, mass and composition of the exploding white dwarf). The identification of a possible second parameter may help us to understand how SNe Ia explode and to improve the calibration of their luminosity. Here we focus on the possible role of a variation of the ratio $R = (^{54}$Fe+^{58}Ni)/^{56}Ni, following a suggestion by Timmes, Brown & Truran (2003).

2 LIGHT CURVE PROPERTIES AND THE ROLE OF THE (^{54}FE+^{58}NI)/^{56}NI RATIO

The peak brightness of a SN Ia is proportional to the mass of ^{56}Ni that is synthesized (Arnett 1982, 1996). In fact, the decay of ^{56}Ni into ^{56}Co and ^{56}Fe produces γ-rays and positrons that deposit their energy in the SN ejecta and eventually cause it to shine. It also follows from simple dimensional analysis that the light-curve width

⋆E-mail: mazzali@mpa-garching.mpg.de

τ_{LC} depends on the ejected mass M_{ej}, the kinetic energy of the explosion E_K, and the grey opacity to optical photons κ_{opt} as

$$\tau_{LC} \propto \kappa_{opt}^{1/2} M_{ej}^{3/4} E_K^{-1/4}. \tag{1}$$

If the white dwarf mass and the explosion energy are assumed to be constant, the shape of the light curve must depend primarily on the opacity. It is now understood (Khokhlov, Müller & Höflich 1993; Höflich et al. 1996) that the two quantities, mass of ^{56}Ni and opacity, are intimately related, so that SN Ia light curves behave to the first order as a one-parameter family.

The thermonuclear explosion that gives rise to a SN Ia (e.g. Nomoto, Thielemann & Yokoi 1984) is thought to produce material that is in nuclear statistical equilibrium (NSE) in the inner parts of the white dwarf. Most of this should be iron-peak nuclei. ^{58}Ni and ^{54}Fe are mainly produced in the innermost ~ 0.2 M$_\odot$, where the density is high enough for weak interactions to be important. In mass shells between ~ 0.2 and ~ 0.8 M$_\odot$, weak interactions operate on a time-scale that is long compared to the nuclear burning time-scale, so that the electron fraction Y_e remains constant in this region during the burning phase; as a consequence, the final relative abundances of ^{58}Ni, ^{56}Ni and ^{54}Fe in this layer are directly related to the value of Y_e at the time of the explosion. The amount of ^{56}Ni produced is essential in determining the brightness of the SN.

Further out still, the densities are too low to burn to NSE, and intermediate-mass elements (IME) such as Si and S are produced. While no γ-rays or positrons are generated here, burning to Si produces almost as much kinetic energy as burning to NSE (Gamezo, Khokhlov & Oran 2005). Therefore this region is also important in determining the properties of the SN. Finally, an outer region consisting of unburned C and O may also exist.

Producing a larger amount of ^{56}Ni leads to more heating. Khokhlov et al. (1993) and Höflich et al. (1996) showed that the opacity increases rapidly with temperature for $T < 10^4$ K, the effective temperature of a typical SN Ia near maximum, but is relatively insensitive to T for higher values. Moreover, since most ^{56}Ni is not mixed, a larger mass of ^{56}Ni does not immediately translate into a higher temperature outside the ^{56}Ni zone.

The explanation of this behaviour lies in the fact that, since continuum processes are depressed in the ejecta of a SN Ia because of the lack of hydrogen and helium, the opacity is dominated by the line opacity of low ionization species (Pauldrach et al. 1996). Combined with the large differential motion of the SN envelope, line absorption causes a pseudo-continuum opacity which is essential in SN Ia light curves. Owing to their complex atomic level structure, ions of Fe-group elements (e.g. Fe II, Fe III, Ni II, Co II, Ti II, Cr II) have many more active lines than IME ions (e.g. Si II, S II) and make the dominant contribution to the line opacity (Mazzali et al. 2001).

Therefore, while producing more ^{56}Ni means producing more photons (i.e. a brighter maximum), the opacity and the shape of the light curve depend on the total amount of NSE material synthesized. The line opacity is in fact the same in different isotopes of the same element, (e.g. ^{56}Fe and ^{54}Fe). Since brighter SNe Ia have broader light curves, the implication is that they do not only make more ^{56}Ni, but also more NSE material. This suggests that brighter SNe do not simply make more ^{56}Ni at the expense of ^{58}Ni or ^{54}Fe.

Mazzali et al. (2001) built parametrized explosion models where the total NSE plus IME content is constant, so that E_K can also be regarded as constant, but different amounts of ^{56}Ni are synthesized at the expense of IME. This was achieved by moving the outer boundary of the ^{56}Ni zone. Synthetic bolometric light-curves of these models reproduced the observed M_{Bol}(Max)–$\Delta m_{15}(B)$ relation (Contardo, Leibundgut & Vacca 2000). Using spectrum synthesis,

Mazzali et al. (2001) showed that the relation between M_B(Max) and $\Delta m_{15}(B)$ can also be recovered.

The role of ^{58}Ni and ^{54}Fe is only to provide an opaque inner zone. Since this zone is very well hidden from the outer layers, the effect of its presence on the early light curve is limited. In this Letter we explore the effect of different R values for the same total mass of NSE material. Timmes et al. (2003) estimate that the final ^{56}Ni mass fraction depends on the initial metallicity Z as $X(^{56}$Ni$) \approx 1 - 0.054\, Z/Z_\odot$, a relation confirmed by detailed three-dimensional explosion and nucleosynthesis calculations by Röpke et al. (2005) and Travaglio, Hillebrandt & Reinecke (2005). Both Höflich, Wheeler & Thielemann (1998) and Dominguez, Höflich & Straniero (2001), using delayed detonation models, also suggest that R increases with the metallicity of the progenitor. They find that their monochromatic and bolometric light-curves are very little affected by changes in R. We explore the dependence in a more systematic way, independent of a specific model of the explosion. Therefore, we consider a situation where ^{58}Ni and ^{54}Fe are present not only at the lowest velocities, where they dominate, but also in the ^{56}Ni zone itself.

3 LIGHT CURVE MODELLING

Mazzali et al. (2001) built parametrized explosion models consisting simply of three zones. The innermost zone (^{54}Fe, ^{58}Ni) only contributes to the opacity. Outside of this, a ^{56}Ni zone produces γ-rays and makes a large contribution to the opacity. The outer zone (IME plus CO) only makes a small contribution to the opacity. They studied three representative explosion models. The models have the same M_{ej}(1.4 M$_\odot$) and E_K ($\sim 1.35 \times 10^{51}$ erg), but contain different amounts of ^{56}Ni: 0.4, 0.6 and 0.8 M$_\odot$, respectively, and were accordingly called Ni04, Ni06 and Ni08. They reproduced the observational properties of SNe 1992A, 1994D and 1990N, which span the range of spectroscopically normal SN Ia decline rates. Starting from those models, we introduced ^{58}Ni and ^{54}Fe in the ^{56}Ni layer in two different amounts, 10 and 20 per cent relative to ^{56}Ni, and with the same distribution, following the predictions of Timmes et al. (2003). We then computed synthetic bolometric light-curves.

The light curves were computed with the grey Monte Carlo code developed by Mazzali et al. (2001). The code follows the propagation and deposition of the γ-ray photons and the positrons emitted in the decay of ^{56}Ni to ^{56}Co and hence to ^{56}Fe. It then follows, also in the Monte Carlo code, the diffusion of the optical photons until they emerge to give rise to the observable SN light. The code adopts a simple parametrization of the line opacity, based on the number of active lines in different elements. In particular, it separates the effect of NSE elements from that of IME and of the original CO of the white dwarf. It also takes into account the decrease of the opacity after maximum caused by the cooling of the ejecta, as described by Khokhlov et al. (1993) and Höflich et al. (1996). The opacity is parametrized as follows:

$$\kappa_{opt} = [0.25 X_{Fe} + 0.025(1 - X_{Fe})] \left(\frac{t_d}{17}\right)^{-\frac{3}{2}} \, [\text{cm}^2 \text{ g}^{-1}], \tag{2}$$

where X_{Fe} is the mass fraction in Fe group elements and t_d the time since the explosion in days. The time-dependent term mimics the effect of the decreasing temperature and is limited to a maximum value of 2.

Since the ^{56}Ni mass of the modified models is smaller by 10 and 20 per cent, respectively, than the original ones, it can be expected that the peak brightness of their respective light curves will be reduced proportionally. However, the effect on the opacity should be very
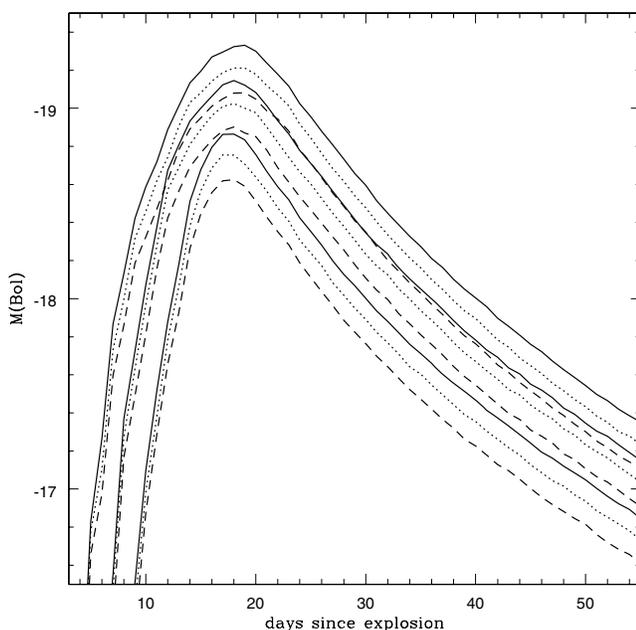
Figure 1. Families of bolometric light-curves computed for models Ni08, Ni06 and Ni04, with and without the inclusion of ^{58}Ni and ^{54}Fe. The continuous curves are for the original models (with 0.8, 0.6 and 0.4 $M_\odot$ of ^{56}Ni, respectively), the dotted ones are for compositions where 10 per cent of ^{56}Ni has been replaced with ^{58}Ni and ^{54}Fe, while in the dashed ones this value is 20 per cent. In all cases, light curves based on model Ni08 are the brightest, while those based on model Ni04 are the dimmest.

Table 1. Parameters of the synthetic light curves.

Model	$M(^{56}\mathrm{Ni})$ [$M_\odot$]	t_{Max} [d]	$M(\mathrm{Bol})_{\mathrm{Max}}$ [mag]	$M(\mathrm{Bol})_{15}$ [mag]	$\Delta m_{15}(\mathrm{Bol})$ [mag]
Ni08	0.80	18.5	−19.33	−18.40	0.93
Ni08-10%	0.72	18.5	−19.21	−18.28	0.93
Ni08-20%	0.64	18.5	−19.08	−18.10	0.92
Ni06	0.60	18.0	−19.15	−18.16	1.01
Ni06-10%	0.54	18.0	−19.03	−18.05	0.98
Ni06-20%	0.48	18.0	−18.90	−17.92	0.98
Ni04	0.40	18.0	−18.87	−17.82	1.05
Ni04-10%	0.36	18.0	−18.76	−17.71	1.05
Ni04-20%	0.32	18.0	−18.63	−17.58	1.05

small: according to equation (2), ^{58}Ni and ^{54}Fe contribute to the opacity as much as ^{56}Ni. In practice, we tested models with different ^{56}Ni masses, but with the same amount and distribution of opacity. The bolometric light curves thus obtained are shown in Fig. 1, and their most important properties are listed in Table 1.

For each set of light curves in Fig. 1, the original light curve is the brightest one. As the ^{58}Ni and ^{54}Fe content increases and the ^{56}Ni content decreases, the light curves become fainter, as expected. However, since models with the same mass of NSE material have similar opacities, their light curves have similar shapes. In contrast, for example, the Ni08-20% model light curve is similar to that of the Ni06 model in peak brightness, but the two light curves have different decline rates. Although the bolometric decline rates are in good agreement with observed values for SNe Ia covering the range of normal spectral properties (Contardo et al. 2000), the occurrence of SNe with different R values can generate a dispersion about the mean $M_{\mathrm{Bol}}(\mathrm{Max}) - \Delta m_{15}(\mathrm{Bol})$ relation. Note that this would not be the case if the changes in composition had been introduced by

extending the inner (^{58}Ni + ^{54}Fe) zone outwards: this would lead to the average location of ^{56}Ni moving outwards as its mass becomes smaller, and hence to a smaller photon diffusion time. This family of light curves would therefore follow the brightness–decline rate relation.

4 EFFECT ON MONOCHROMATIC DECLINE RATES

Our bolometric light-curves were produced using a simple code, the main advantages of which is that it makes it easy to trace the effect of properties such as the ^{56}Ni distribution and that it is not subject to uncertainties arising from the use of opacity tables. Obviously, it would be very interesting to verify how the monochromatic light curves are affected, as these are directly observable. As was done in Mazzali et al. (2001), we checked the behaviour of the monochromatic bands computing spectra at the appropriate epochs (maximum and 15 d later) with our Monte Carlo spectrum synthesis code (Mazzali & Lucy 1993; Lucy 1999; Mazzali 2000). The bolometric luminosities and the photospheric velocities obtained from our synthetic light curves were used as input for the spectral calculations.

The results for the spectra at maximum are shown in Table 2. Interestingly, although the luminosity of the models with a higher ^{58}Ni and ^{54}Fe content is smaller than that of the original models, the colours of the spectra are essentially unchanged, i.e. both B and V change by roughly equal amounts. This confirms the findings of Höflich et al. (1998) and Dominguez et al. (2001) and provides further support to the notion that the typical colour of normal SNe Ia at maximum light is $(B - V) \sim 0.0$–0.1. Furthermore, the brightest SNe (model Ni08) are not the bluest. This is due to the changing ionization conditions, with strong Fe III lines developing in the B band. This change from Fe II to Fe III does not affect the light curve much: opacity is shifted to the blue, but so is the average flux because the temperature is higher. Originally, the three spectra resembled those of SNe 1992A, 1994D and 1990N, respectively (Mazzali et al. 2001, fig. 5). The spectra of the modified models are very similar, except for an offset in flux and a slight reduction in temperature as the mass of ^{56}Ni is reduced.

The shape of the synthetic spectra 15 d after maximum depends sensitively on the choice of photospheric velocity, which is very uncertain at such advanced epochs. This affects in particular the B magnitudes and the $B - V$ colour. However, small changes to lower velocities than those predicted by the light curve code are sufficient to obtain spectra with $\Delta m_{15}(B)$ values similar to the original models. On the other hand, the V magnitude is almost unaffected by the choice of photospheric velocity within this range. Therefore, the value of $\Delta m_{15}(V)$ can be determined quite accurately. We

Table 2. Properties of the spectra and inferred value of the decline rates.

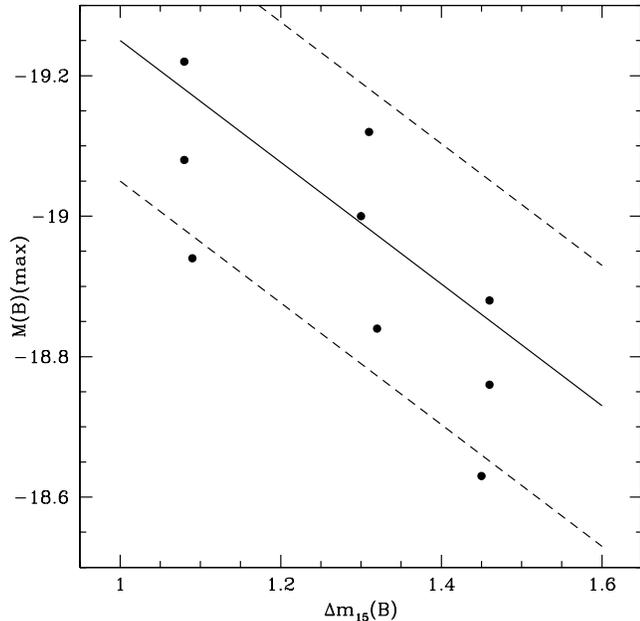| Model	$M(B)_{\mathrm{Max}}$ [mag]	$(B - V)_{\mathrm{Max}}$ [mag]	$(B - V)_{15}$ [mag]	$\Delta m_{15}(B)$ [mag]	$\Delta m_{15}(V)$ [mag]
Ni08	−19.22	0.10	0.56	1.08	0.62
Ni08-10%	−19.08	0.10	0.61	1.08	0.57
Ni08-20%	−18.94	0.16	0.65	1.09	0.60
Ni06	−19.12	0.06	0.70	1.31	0.67
Ni06-10%	−19.03	0.08	0.71	1.30	0.67
Ni06-20%	−18.85	0.08	0.79	1.32	0.61
Ni04	−18.88	0.06	0.81	1.46	0.71
Ni04-10%	−18.76	0.06	0.84	1.46	0.68
Ni04-20%	−18.63	0.07	0.81	1.45	0.71

Figure 2. The position of the models on the brightness–decline rate diagram. The ridge line is the locus of the Calan–Tololo SNe (Hamuy et al. 1996a), shifted for $H_0 = 72 \text{ km s}^{-1} \text{ Mpc}^{-1}$, and the dashed lines are the 1σ dispersion.

computed $\Delta m_{15}(V)$ rather than $\Delta m_{20}(V)$, the value measured by Hamuy et al. (1996b), because the position of the photosphere would be even more uncertain at a later epoch. The values of $\Delta m_{15}(V)$ for our model set (Table 2) compare well with those of observed SNe Ia (Hamuy et al. 1996b, table 1). Since $\Delta m_{15}(B)$ and $\Delta m_{20}(V)$ are observationally very well correlated (Hamuy et al. 1996b), the agreement between our computed values of $\Delta m_{15}(V)$ and the observed ones supports our hypothesis that $\Delta m_{15}(B)$ does also not change significantly with R.

Our calculations confirm that SNe with constant total NSE content but $(^{58}\text{Ni} + {}^{54}\text{Fe})/{}^{56}\text{Ni}$ ratios that are varying within the range suggested by Timmes et al. (2003) span a range of ∼0.25 mag in peak brightness. However, they have similar V- and B-band decline rates. If SNe with a variable R do exist, they would show a scatter in the peak magnitude–decline rate diagram comparable to the observed one. This is illustrated in Fig. 2, where we plot the location of our models in this diagram and the spread of observed SN properties: our models are able to reproduce both the brightness–decline relation and the observed scatter. This suggests that R may be one of the most important parameters responsible for the dispersion in the brightness–decline rate relation.

More accurate pre-SN calculations and detailed explosion models may be able to determine the value and range of the ratio $(^{58}\text{Ni} + {}^{54}\text{Fe})/{}^{56}\text{Ni}$ depending on the properties of the progenitor white dwarf such as metallicity or age (cf. Lesaffre et al. 2006). At the same time, it will be important to verify the observable effect the ratio has on the observable properties of a SN Ia with more accurate radiative transfer calculations. Quantifying the effect and correcting for this may ultimately lead to a reduction of the scatter in the peak brightness–decline rate relation. A way to separate the first and the second parameter for nearby SNe could be the follow-

ing. On the one hand, the mass of ^{56}Ni can be derived from the late light-curves, when the SN brightness is more directly sensitive to γ-ray and positron deposition. On the other hand, nebular spectra could be used to obtain information on both the mass of ^{56}Ni and that of non-radioactive Fe-group isotopes.

REFERENCES

Arnett D., 1982, ApJ, 253, 785
Arnett D., 1996, Supernovae and Nucleosynthesis. Princeton Universus Press, Princeton
Benetti S. et al., 2004, MNRAS, 348, 261
Branch D., Romanishin W. Baron E., 1996, ApJ, 467, 473
Contardo G., Leibundgut B., Vacca W. D., 2000, A&A, 359, 876
Dominguez I., Höflich P., Straniero O., 2001, ApJ, 557, 279
Gamezo V., Khokhlov A. M., Oran E., 2005, ApJ, 623, 337
Hamuy M., Phillips M. M., Schommer R. A., Suntzeff N. B., Maza J., Aviles R., 1996a, AJ, 112, 2391
Hamuy M., Phillips M. M., Suntzeff N. B., Schommer R. A., Maza J., Smith R. C., Lira P., Aviles R., 1996b, AJ, 112, 2438
Hamuy M., Trager S. C., Pinto P. A., Phillips M. M., Schommer R. A., Ivanov V., Suntzeff N. B., 2000, AJ, 120, 1479
Höflich P., Khokhlov A. M., Wheeler J. C., Phillips M. M., Suntzeff N. B., Hamuy M., 1996, ApJ, 472, L81
Höflich P., Wheeler J. C., Thielemann F. K., 1998, ApJ, 495, 617
Khokhlov A., Müller E., Höflich P., 1993, A&A, 270, 223
Lesaffre P., Han Z., Tout C. A., Podsiadlowski Ph., Martin R. G., 2006, MNRAS, in press (doi:10.1111/j.1365-2966.2006.10068.x) (astro-ph/0601443)
Lucy L. B., 1999, A&A, 345, 211
Mazzali P. A., 2000, A&A, 363, 705
Mazzali P. A., Lucy L. B., 1993, A&A, 279, 447
Mazzali P. A., Cappellaro E., Danziger I. J., Turatto M, Benetti S., 1998, ApJ, 499, L49
Mazzali P. A., Nomoto K., Cappellaro E., Nakamura T., Umeda H., Iwamoto K., 2001, ApJ, 547, 988
Nomoto K., Thielemann F.-K., Yokoi K., 1984, ApJ, 286, 644
Nugent P., Phillips M., Baron E., Branch D., Hauschild P. H., 1995, ApJ, 455, L147
Pauldrach A. W. A., Duschinger M., Mazzali P. A., Puls J., Lennon M., Miller D. L., 1996, A&A, 312, 525
Perlmutter S. et al., 1997, ApJ, 483, 565
Phillips M. M., 1993, ApJ, 413, L105
Phillips M. M., Lira P., Suntzeff N. B., Schommer R. A., Hamuy M., Maza J., 1999, AJ, 118, 1766
Riess A. G. et al., 1998, AJ, 116, 1009
Röpke F., Gieseler M., Reinecke M., Travaglio C., Hillebrandt W., 2005, A&A, submitted (astro-ph/0506107)
Timmes R., Brown E. F., Truran J. W., 2003, ApJ, 590, L83
Travaglio C., Hillebrandt W., Reinecke M., 2005, A&A, 443, 1007
van den Bergh S., 1997, AJ, 113, 1
van den Bergh S., Li W., Filippenko A. V., 2005, PASP, 117, 773
Wang L., Höflich P., Wheeler J. C., 1997, ApJ, 476, L27
Wang X., Wang L., Zhou X., Lou Y.-Q., Li Z., 2005, ApJ, 620, L87

This paper has been typeset from a TeX/LaTeX file prepared by the author.